Nuclear theory – Nuclear astrophysics

J.W. Holt

Introduction:

The structure, phases, and dynamics of nuclear matter are crucial to understand stellar explosions, the origin of the elements, patterns in observed gravitational waves, and the composition of the densest observable matter in the universe. The appropriate tool to study strongly interacting matter at the typical scales relevant in nuclear astrophysics (well below the scale of chiral symmetry breaking $\Lambda_\chi \approx 1$ GeV) is chiral effective field theory [WEI79, EPE09, MAC11]. In recent years, chiral effective field theory has become a cornerstone of the modern approach to nuclear many-body dynamics that provides a systematic framework for describing realistic microphysics, such as multi-pion exchange processes and three-body forces, within a well-defined organizational hierarchy. The long and intermediate-range parts of the nuclear potential result from one- and two-pion exchange processes, while short-distance dynamics, not resolved at the wavelengths corresponding to typical nuclear Fermi momenta, are introduced as contact interactions between nucleons. Chiral effective field theory is unique in its multichannel methods for quantifying uncertainties and especially in its ability to estimate the importance of missing physics.

Radius and equation of state constraints from massive neutron stars and GW190814

In June 2020, the LIGO/Virgo Collaboration reported measurements [ABB20] of gravitational waves resulting from a $2.50 - 2.67 M_\odot$ "mass-gap" object in binary coalescence with a heavy $22.2 - 24.3 M_\odot$ companion black hole. Taken at face value, the mass-gap secondary object in the observation represents the discovery of either the heaviest known neutron star (NS) or the lightest known black hole (BH). Motivated by the unknown nature of the $2.50 - 2.67 M_\odot$ compact object in the binary merger event GW190814, we have studied [LIM20] the maximum neutron star mass based on constraints from low-energy nuclear physics, neutron star tidal deformabilities from GW170817, and simultaneous mass-radius measurements of PSR J0030+045 from NICER. Our prior distribution is based on a combination of nuclear modeling valid in the vicinity of normal nuclear densities together with the assumption of a maximally stiff equation of state at high densities, a choice that enables us to probe the connection between observed heavy neutron stars and the transition density at which conventional nuclear physics models must break down. We have demonstrated that a modification of the highly uncertain supra-saturation density equation of state beyond 2.64 times normal nuclear density is required in order for chiral effective field theory models to be consistent with current neutron star observations and the existence of $2.6 M_\odot$ neutron stars. We have also shown that the existence of very massive neutron stars strongly impacts the radii of $\sim 2.0 M_\odot$ neutron stars. In Fig. 1 we show the critical density n_t beyond which traditional nuclear physics modeling must break down in order to support neutron stars with mass $M_{\rm max}$.

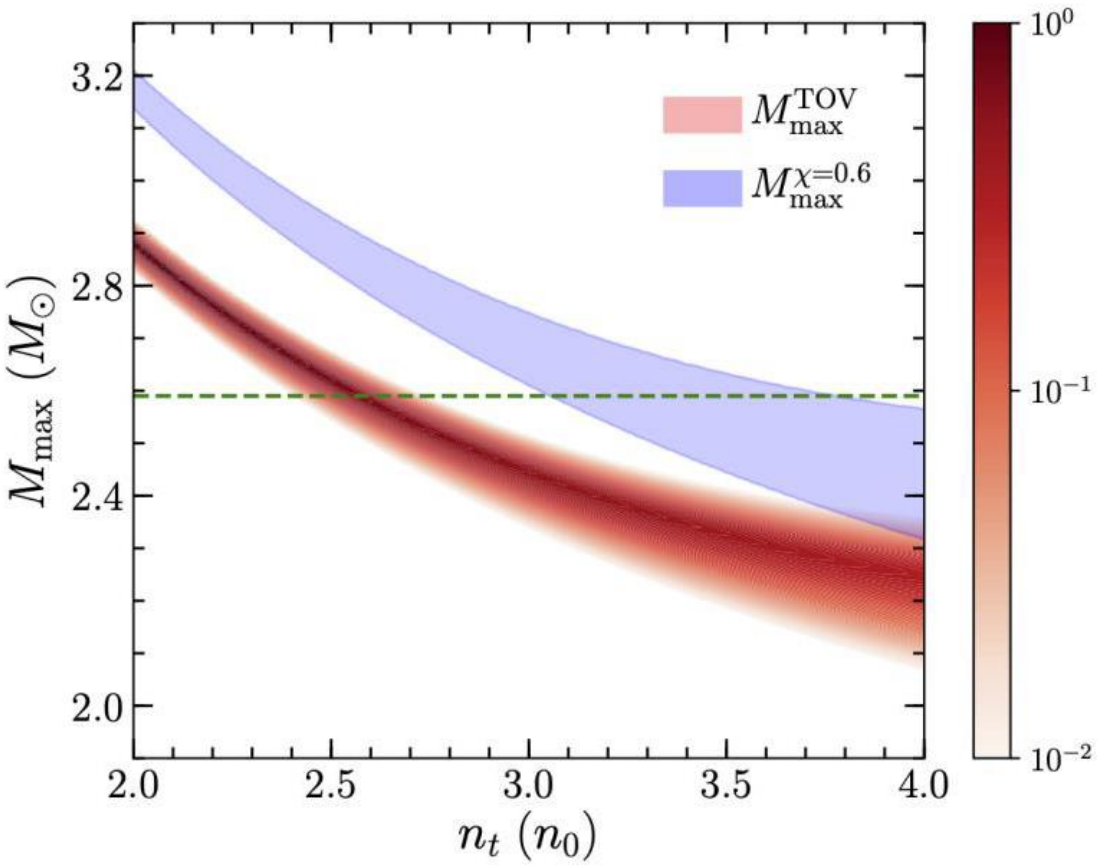

Fig. 1. Minimum transition density $\boldsymbol{n_t}$ at which traditional nuclear physics models break down in order to support massive $\boldsymbol{M}_{\rm max}$ neutron stars. Shown also is the same quantity in the case of rapidly rotating neutron stars with spin $\boldsymbol{\chi = 0.6}$.

Microscopic global optical potential from chiral effective field theory

Numerical simulations of r-process nucleosynthesis are essential for identifying the astrophysical site of the r-process, the primary candidates being the wind-driven ejecta from accretion disks surrounding binary neutron-star mergers or collapsars as well as the neutrino-driven winds of core-collapse supernovae. Neutron-capture rates on exotic neutron-rich isotopes are particularly important during the non-equilibrium freeze-out phase of r-process nucleosynthesis, but direct experimental studies at rare-isotope facilities remain unfeasible. The large uncertainties in these capture rates, due in part to difficulties in extrapolating phenomenological optical model potentials far from the valley of stability, limit the precision of predicted heavy-element abundances. Previously we have computed proton-nucleus and neutron-nucleus optical potentials [WHI19,WHI20] by combining the improved local density approximation with chiral effective field theory calculations of the nucleon self energy in homogeneous nuclear matter. Differential elastic scattering cross sections on calcium isotopes were found to be in quite good agreement with experimental data for projectile energies up to 150 MeV.

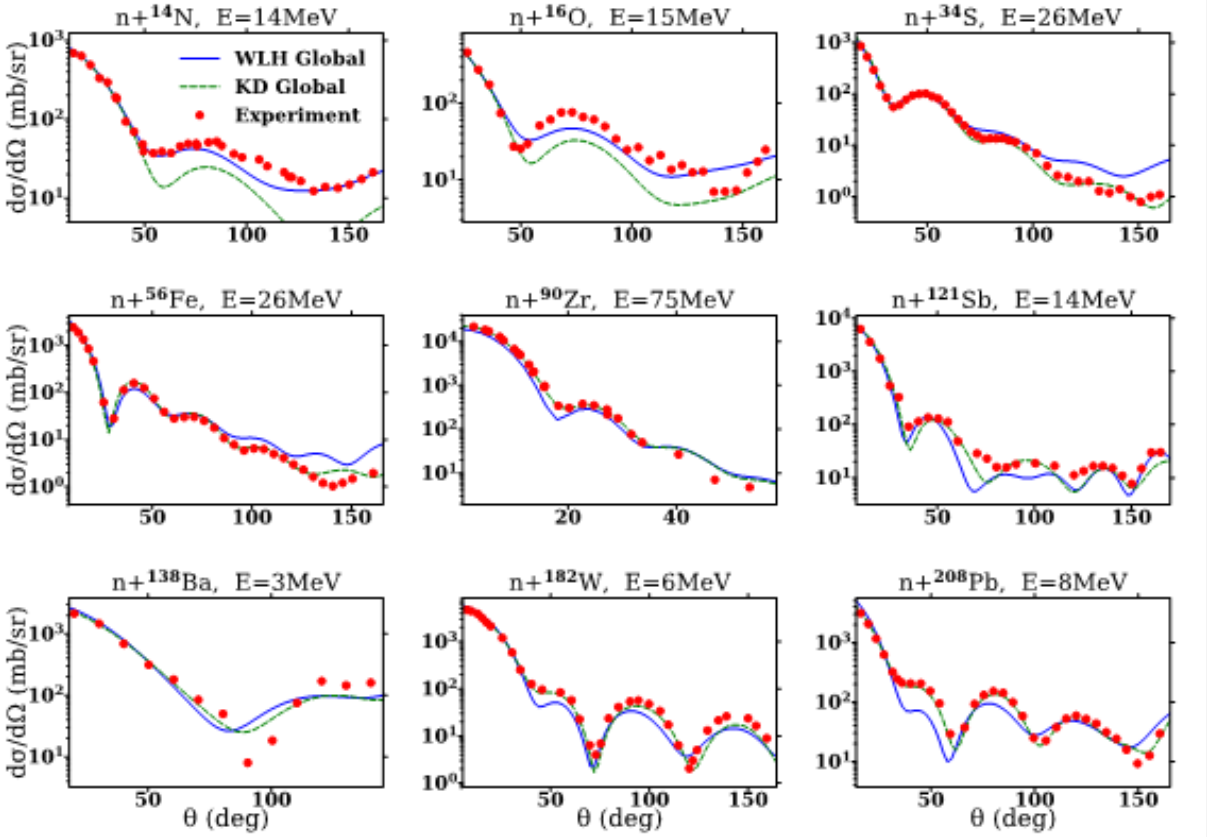

Fig. 2. Neutron elastic differential scattering cross sections from the microscopic global optical potential of Ref. [WHI21] (blue) compared to experimental data (red dots) and the Koning-Delaroche phenomenological optical potential (green dashed).

Recently, we have constructed from chiral effective field theory two- and three-body forces a microscopic global nucleon-nucleus optical potential suitable for reactions involving radioactive isotopes. Within the improved local density approximation and without any adjustable parameters, we have computed local proton and neutron optical potentials for 1800 target nuclei in the mass range $12 < A < 242$ and for energies between $0\ \text{MeV} < E < 200\ \text{MeV}$. We then constructed a global optical potential parametrization that depends smoothly on the projectile energy as well as the target nucleus mass number and isospin asymmetry. Elastic scattering observables calculated from the global optical potential were found to be in good agreement with available experimental data for a wide range of projectile energies and target nuclei. In Fig. 2 we show the predicted neutron elastic differential scattering cross sections for a range of isotopes and energies from the microscopic global optical potential of Ref. [WHI21] compared to experimental data and the results from the Koning-Delaroche phenomenological optical potential [KON03].

Constraining the nonanalytic terms in the isospin-asymmetry expansion of the nuclear equation of state

The equation of state of nuclear matter at arbitrary proton fraction and density is crucial for understanding the structure and dynamics of neutron stars, the properties of neutron-rich nuclei, and data from terrestrial heavy-ion collision experiments. We have extracted [WEN21] from chiral two- and three-body forces the high-order symmetry energy coefficients that consist of both normal terms (occurring with even powers of the isospin asymmetry δ) and terms involving the logarithm of the isospin asymmetry that are formally nonanalytic around the expansion point of isospin-symmetric nuclear matter:

$$\bar{E}(n,\delta) = A_0(n) + A_2(n)\delta^2 + \sum_{i>1}\left(A_{2i}(n) + A_{2i,l}(n)\log|\delta|\right)\delta^{2i}.$$

The coefficients were extracted from numerically precise perturbation theory calculations of the equation of state coupled with a new set of finite difference formulas that achieve stability by explicitly removing the effects of higher-order terms in the expansion. We have found that the coefficients of the logarithmic terms are generically larger in magnitude than those of the normal terms from second-order perturbation theory diagrams, but overall the normal terms give larger contributions to the ground state energy. We have also observed that high-order isospin-asymmetry terms are especially relevant at large densities where they effect the proton fraction in beta-equilibrium matter. In Fig. 3 we plot the density dependence of the coefficients A_4, A_6, A_{4l}, A_{6l} in the modified isospin-asymmetry expansion of the nuclear EOS arising at second-order in perturbation theory. We consider as an estimate of the theoretical uncertainty five different chiral potentials and include three-body forces throughout.

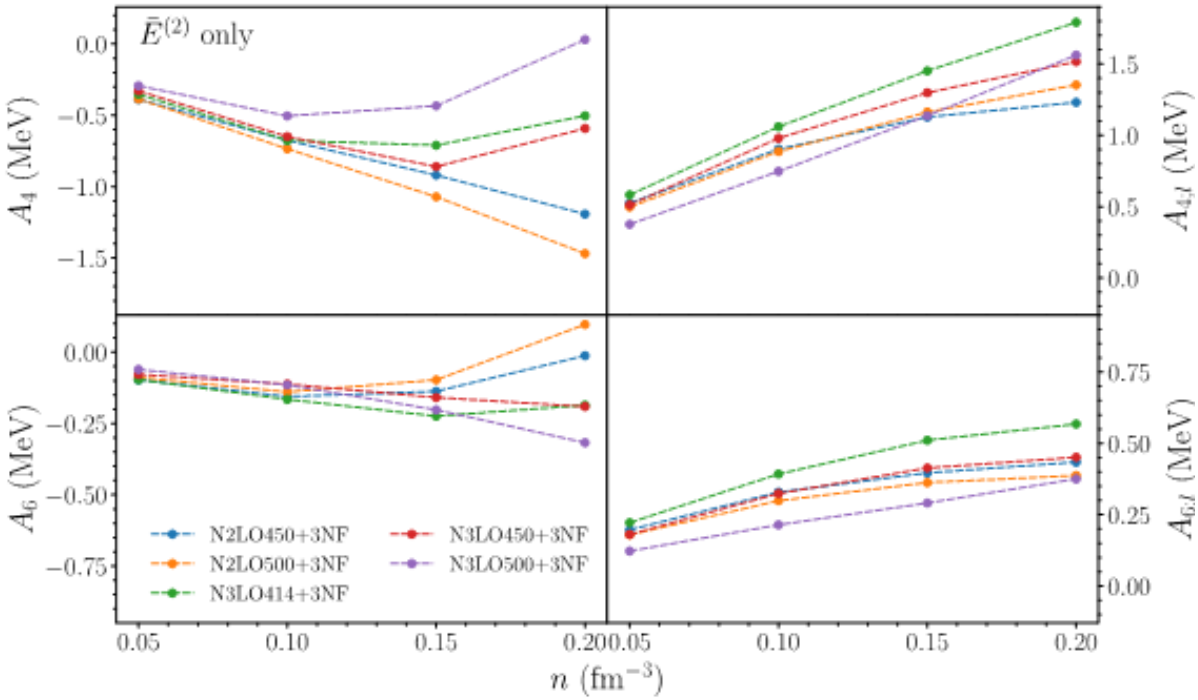

Fig. 3. Density dependence of the high-order normal and logarithmic contributions to the isospin-asymmetry dependence of the nuclear equation of state from chiral effective field theory two-body and three-body forces.

[1] S. Weinberg, Physica A **96**, 327 (1979).
[2] E. Epelbaum, H.-W. Hammer and U.-G. Meissner, Rev. Mod. Phys. **81**, 1773 (2009).
[3] R. Machleidt and D. R. Entem, Phys. Rept. **503**, 1 (2011).
[4] R. Abbott *et al.* (LIGO Scientific Collaboration and Virgo Collaboration) Astrophys. J. Lett. **896**, L44 (2020).
[5] Y. Lim, A. Bhattacharya, J.W. Holt, and D. Pati, arXiv:2007.0652.
[6] T.R. Whitehead, Y. Lim, and J.W. Holt, Phys. Rev. C **100**, 014601 (2019).
[7] T.R. Whitehead, Y. Lim, and J.W. Holt, Phys. Rev. C **101**, 064613 (2020).
[8] T.R. Whitehead, Y. Lim, and J.W. Holt, arXiv:2009.08436.
[9] A.J. Koning and J.P. Delaroche, Nucl. Phys. **A713**, 231 (2003).
[10] P. Wen and J.W. Holt, Phys. Rev. C **103**, 064002 (2021).